Macromolecular Research, Vol. 17, No. 12, pp 987-994 (2009)

Hybrid Nanocomposites of Palladium Nanoparticles Having POSS and MWNTs via Ionic Interactions

Jong-hwan Jeon, Jung-hyurk Lim, and Kyung-min Kim*

Department of Polymer Science and Engineering, Chungju National University, Chungbuk 380-702, Korea

Received April 8, 2009; Revised July 6, 2009; Accepted July 6, 2009

Abstract: Palladium nanoparticles having cubic silsesquioxanes (POSS) (Pd-POSS) were produced by the reaction of palladium (II) acetate and octa(3-aminopropyl)octasilsesquioxane octahydrochloride (POSS-NH_3^+) in methanol at room temperature. Functionalized multiwalled carbon nanotubes (MWNT-COOH) were prepared by acid treatment of pristine MWNTs. The hybrid nanocomposites of Pd-POSS and MWNT-COOH (Pd-MWNT nanocomposites) were synthesized by self-assembly method via ionic interaction between positively charged Pd-POSS and negatively charged MWNT-COO^-. The spherical aggregates of Pd-POSS with a diameter of 40-60 nm were well attached to the surfaces of MWNT-COOH on Silicon wafer. The composition, structure, and surface morphology of Pd-MWNT nanocomposites were studied by UV-vis spectrophotometer, energy dispersive spectrum (EDX), scanning electron microscopy (SEM), and atomic force microscope (AFM).

Keywords: palladium nanoparticles, multiwalled carbon nanotube, self-assembly, hybrid nanocomposites, surface modification.

Introduction

Architectural control of metal nanostructures has been of immerse interest for various applications. The size, shape, composition, crystallinity, and structure of the metal nanostructures determine their properties. Metal nanoparticles have unique chemical and physical properties, such as catalytic, optical, and magnetic properties comparing to those of bulk metals or atoms.[1-4] Multiscale organization of the metal nanoparticles with a controlled manner is attractive for the application of a molecular system in macroscopic devices[5,6] as well as for the creation of structured systems at molecular level.[7-13] Carbon nanotubes (CNTs) have been studied for a lot of potential applications due to their outstanding physical properties.[14-23] Functionalized CNTs have generated great interest for dispersion enhancement in processing or for chemical modifications.[24,25] Shortening of carbon nanotubes by ultrasonication with oxidizing acid mixtures is frequently used to functionalize CNTs.[26]

CNT/nanoparticle complexes can be used in fuel cells or sensors. The recent interest is focused on the templates for nanotrees based on CNT/nanoparticle complexes.[27-29] There are various approaches for CNT/nanoparticle complexes such as physical evaporation, chemical reaction with functionalized CNTs, and electroless deposition method.[26,27,30-32] The incorporation of the metal nanoparticles to the surfaces of CNTs have been useful method to obtain hybrid nanocomposites with useful properties.[33] It is essential to activate their surfaces for attaching novel metal nanoparticles to the side wall of CNTs because the surfaces of carbon nanotube are inert.[34,35] The surface modification of CNTs with organic functional group is widely used for anchoring novel metal nanoparticles onto CNTs.[36-38] Palladium nanoparticles can be attached on noncovalently functionalized CNTs. Reports are available on various CNTs modified with palladium nanoparticles through electron beam evaporation, thermal evaporation, and sputtering for hydrogen detection. Palladium has been used as catalyst for various applications.[39-42] Palladium has shown its potential for applications in various fields of engineering and technology including catalysis[39-42] and hydrogen storage.[43-48] Palladium is also used as catalysts for the gas sensors[49-51] and has been used as catalytic material for the synthesis of carbon nanotubes.[40,52] The carbon nanotubes loaded with palladium nanoparticles have been used for the detection of methane.[53] Palladium nanostructures with different shapes and sizes can make the surface occurring phenomenon more interesting.

In this study, hybrid nanocopmposites of palladium nanoparticles having silsesquioxanes (Pd-POSSS) and MWNT-COOH were prepared by self-assembly method via ionic interaction between positively charged Pd-POSS and negatively charged MWNT-COO^-. The spherical aggregates of palladium nanoparticles (Pd-POSS) were synthesized by using the cubic silsesquioxanes (POSS-NH_3^+) as a cross-linker

*Corresponding Author. E-mail: kmkim@chungju.ac.kr

for the self-organization of the individual palladium nanoparticles.[56] Functionalized carbon nanotubes (MWNT-COOH) were prepared by acid treatment in H_2SO_4/HNO_3 mixture. To our knowledge, there was no report on hybrid nanocomposites of Pd-POSS and MWNT-COOH (Pd-MWNT nanocomposites) via electrostatic interaction as physical interaction. New Pd-MWNT nanocomposites could be ideal hydrogen sensing materials as compared with conventional materials containing individual palladium nanoparticles due to the higher amount of palladium nanoparticles derived from the deposition of spherical aggregates of Pd-POSS onto the surfaces of MWNTs. Additionally, hybrid nanocomposites of MWNT-COOH and spherical aggregates of palladium nanoparticles having dendrimer instead of POSS-NH_3^+ will be fabricated to observe the hydrogen sensing property. Continuous research is going on to study the fabrication of hydrogen storage and sensing devices using Pd-MWNT nanocomposites. Using this new concept, we can also demonstrate the deposition of conducting polymers on the surfaces of MWNT-COOH and fabricate hybrid nanocomposites of Pd-POSS and various polymers. In this system, POSS-NH_3^+ acts as a cross-linker for the palladium nanoparticles to construct Pd-POSS, and MWNT-COOH are used for Pd-POSS to make hybrid nanocomposites. FE-SEM and AFM studies showed that the complex formation of Pd-POSS with a diameter of 40-60 nm and MWNT-COOH was successfully achieved and Pd-POSS were nicely dispersed on the surfaces of MWNT-COOH on Silicon wafer.

Experimental

Materials. Pristine MWNTs were obtained from the Iljin Nanotech Inc (diameter: 10-20 nm, length: 10-50 μm, >90 vol% of purity). (3-Aminopropyl)triethoxysilane was purchased from Aldrich. *N*-(2–aminoethyl)-11-aminoundecyltrimethoxysilane was purchased form Gelest. Hydrochloric acid (HCl), nitric acid (HNO_3), sulfuric acid (H_2SO_4), methanol (MeOH), sodium hydroxide (NaOH), acetone, tetrahydrofuran (THF), chloroform, and ethanol were obtained from Aldrich.

Measurements. Fourier transform infrared (FTIR) spectra (FTS-6000, BIO-RAD) and Raman spectro-photometer (NRS-3200, JASCO) were used to confirm and characterize MWNT-COOH which was formed after chemical modification of pristine MWNTs under acidic condition. The dispersions of pristine MWNTs and MWNT-COOH in aqueous media were measured by using the camera (D40, NIKON). The thermal behavior was examined by thermogravimetric analysis (TGA) (TGA S-1000, SCINCO) under atmosphere. Surface electro optics (contact angle) (PHEOENIX-300) and UV-vis spectro-photometer (OPTIZEN 2120UV, MECASYS) were used to observe the surface property. The morphologies and structures were observed by atomic force microscope (AFM) (XE-1000, PARK SYSTEMS), scanning electron microscopy (SEM) (JSM-6700, JEOL), and energy dispersive spectrum (EDX).

Synthesis of Octa(3-aminopropyl)octasilsesquioxane Octahydrochloride (POSS-NH_3^+) (Scheme I). The reaction of $H_2NCH_2CH_2CH_2Si(OEt)_3$ (150 mL, 0.627 mol) and conc. HCl (200 mL) in MeOH (3.6 L) produces octa(3-aminopropyl)octasilsesquioxane octahydrochloride (30%) as a microcrystalline solid after 6 weeks at 25 °C. The crude product obtained after filteration, washing with MeOH, and drying (0.001 torr, 25 °C) is spectroscopically pure. Recrystallization from MeOH affords octa(3-aminopropyl)octasilsesquioxaneoctahydro chloride as a white microcrystalline powder.[54]

Acid Treatment of Pristine MWNTs (Scheme II). Typically, 6.0 g of crude MWNTs, 50 mL of 60% HNO_3, and 150 mL of 98% H_2SO_4 were added into a 500 mL flask equipped with a condenser under vigorous stirring. The flask was then immersed in a sonication bath (40 kHz) for

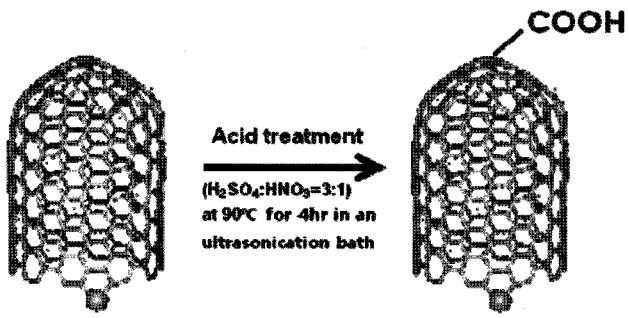

Scheme II. Chemical modifications of the pristine MWNTs.

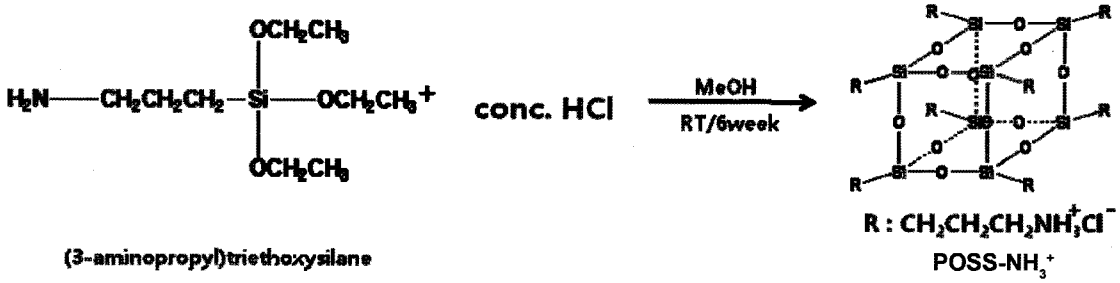

(3-aminopropyl)triethoxysilane

Scheme I. Synthesis of octa(3-aminopropyl)octasilsesquioxane octahydrochloride (POSS-NH_3^+).

90 min. The mixture was then stirred for 3 h under reflux (90 °C). During this period, densely brown gas was collected and treated with a NaOH aqueous solution connected to the condenser by a plastic tube. After cooling to room temperature, the reaction mixture was diluted with 500 mL of deionized water and then vaccum-filtered through a filter paper. The dispersion, filtering, and washing steps were repeated until the pH of the filtrate reached 7 (at least four cycles were required). The filtered solid was then washed with ca. 100 mL of acetone and THF at 5 times to remove most of the water from the sample and dried under vacuum for 24 h at 60 °C.[55]

The Dispersions of Pristine MWNTs and MWNT-COOH with Different Size in Aqueous Media. To confirm the surface modification of MWNTs for good deposition of Pd-POSS, the dispersions of MWNT-COOH with different size in aqueous media were prepared with four types of MWNTs (length of MWNTs: 0.2 μm, 1 μm, 3 μm, and 5 μm). For each experiment, the concentration of MWNTs (each pristine and MWNT-COOH for 0.2~5 μm length) in the DDI water was 0.0001 g/mL. The resulting mixture was ultrasonicated by using a bath-type ultrasonicator.

Preparation of Spherical Aggregates of Palladium Nanoparticles Having POSS (Pd-POSS). When a methanol solution (50 mL) of octa(3-aminopropyl)octasilsesquioxane (10 mg) and palladium(II) acetate (20 mg) was stirred at room temperature, the solution immediately became turbid. The turbid solution gradually turned from yellow to black with increasing the reaction time, indicating the reduction of the palladium ions. The resulting black colloidal solution was stable and neither precipitated nor flocculated over a period of several months.[56] The average size of Pd-POSS was 40-60 nm measured by the scanning electron microscopy (SEM) and atomic force microscope (AFM) images.

Deposition of Pd-POSS on MWNT-COOH of the Silicon Wafer (Pd-MWNT Nanocomposites) (Scheme III). Prior to this experiment, Si-wafer was cleaned with chloroform by using the ultrasonicator, and then treated with piranha and plasma ($Ar+O_2$ gas). As a result, the hydrophilic layer was formed on the surfaces of the Si-wafer. Hydroxy-functionalized substrates were dipped into the ethanol solution of *N*-(2-aminoethyl)-11-aminoundecyltrimethoxysilane and were taken out. After that, substrates were immersed in DDI water solution of MWNT-COOH for 12 h to coat the MWNT-COOH on the amine-functionalized substrates by self-assembly reaction. Then the substrates were immersed in methanol solution of POSS-NH_3^+ and palladium (II) acetate with changing the reaction time for electrostatic interaction between positively charged Pd-POSS and negatively charged MWNT-COO^-. For the comparison of the result, MWNT-COOH on silicon wafer were also immersed in methanol solution of palladium (II) acetate which made individual palladium nanoparticles with no POSS-NH_3^+.

Results and Discussion

Figure 1 shows the FTIR spectra of pristine MWNTs, MWNT-COOH, Pd-POSS, and hybrid nanocomposites of Pd-POSS and MWNT-COOH (Pd-MWNT nanocomposites). The spectrum of the pristine MWNTs shows a C=C stretching peak at 1632 cm^{-1}. It, however, shows no discernable peak, indicating the formation of carboxylic acids or defects after purification. The C=C stretching peaks, which indicate graphite structure of MWNTs, are observed in the MWNT-COOH as well. After acid treatment, MWNT- COOH show a C=O stretching peak from the COOH group at 1714 cm^{-1} and a very broad O-H stretching peak between 3200 and

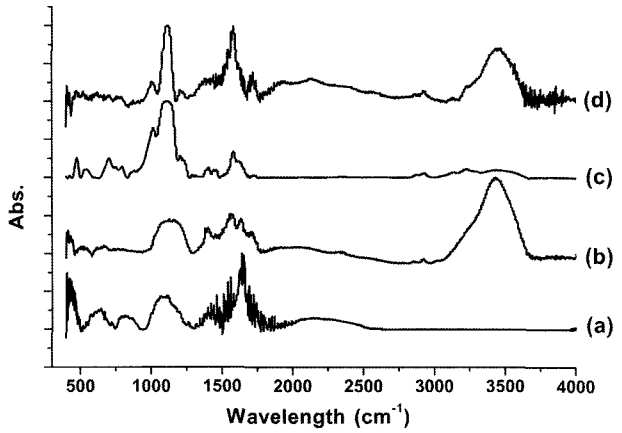

Figure 1. FTIR spectra of pristine MWNTs (a), MWNT-COOH (b), Pd-POSS (c), and Pd-MWNT nanocomposites (d).

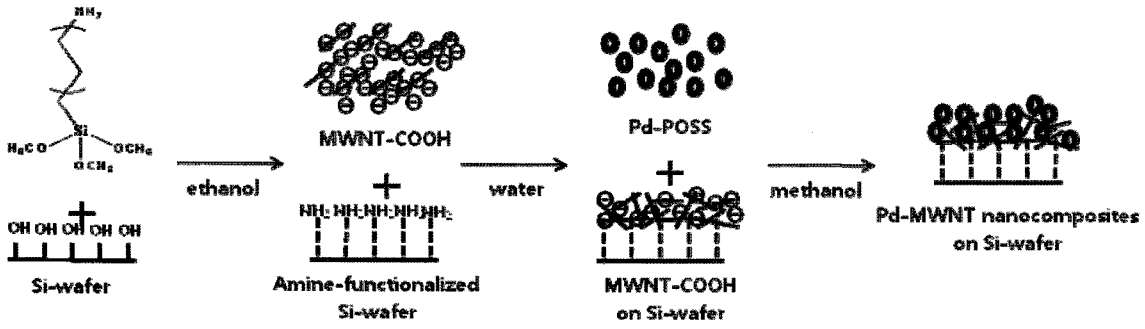

Scheme III. Schematic illustration of the experimental procedures for Pd-MWNT nanocomposites.

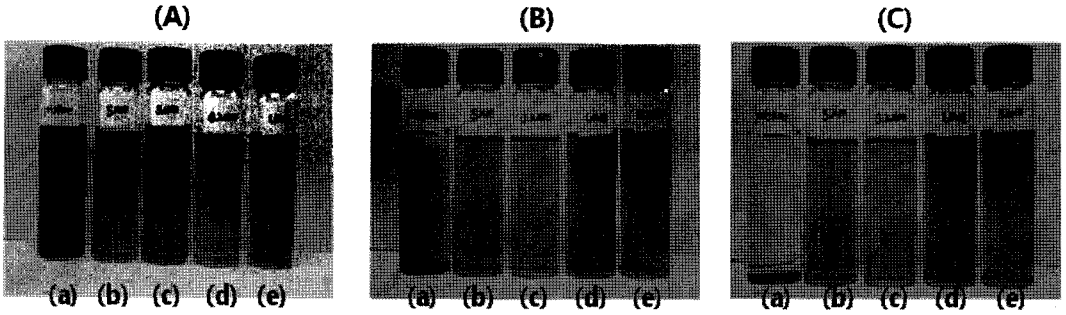

Figure 2. Photographic images of pristine MWNTs and MWNT-COOH in aqueous media after 1 h (A), 1 day (B), and 2 weeks (C): pristine MWNTs (a) and MWNT-COOH (various lengths) (b-e).

3600 cm^{-1}. Pd-POSS show a NH_3^+ peak and Si-O-Si peak derived from POSS-NH_3^+ at 3227 cm^{-1} and 1110 cm^{-1}, respectively. Pd-MWNT nanocomposites show a C=O stretching peak at 1719 cm^{-1} and Si-O-Si peak at 1108 cm^{-1}.

Figure 2 shows the dispersion photographic images of pristine MWNTs and MWNT-COOH with different length in aqueous media after 1 h, 1 day, and 2 weeks. The concentration of various MWNTs in the water was 0.0001 g/mL. All MWNTs show good dispersion in aqueous media at room temperature as shown in Figure 2(A). Figure 2(B) and (C) reveal still good dispersion stability at room temperature except pristine MWNTs (refer to (a) in Figure 2(B) and 2(C)) with increasing the storage time.

Raman spectroscopy is a powerful tool used to characterize the functionalized CNTs. The typical Raman spectra for the MWNTs consist of two quite sharp modes, the G band around 1580 cm^{-1} and the D band around 1350 cm^{-1} accompanied by an additional D' band as shoulder to the G band at crystalline graphite carbon in MWNTs, whereas the D band is originated from the disorder induced features. The presence of the D' band at 1612 cm^{-1} is affected by the disorder in MWNTs, which can be barely observable in pristine MWNTs but is clearly detectable after functionalization of MWNTs. As shown in Figure 3(a), the D and G band of pristine MWNTs show at nearly 1350 cm^{-1} and 1580 cm^{-1}, respectively. After acid treatment of MWNTs, the G band was shifted a little bit in the position of Raman peaks and D' band was observed at 1612 cm^{-1}, indicating an increase in defects along the MWNT body. The ratio of the intensity of the disordered to ordered transition, which indicates the generation of surface defects due to the functionalization of MWNTs, increases from 0.99 (pristine MWNTs) to 1.02 (MWNT-COOH).

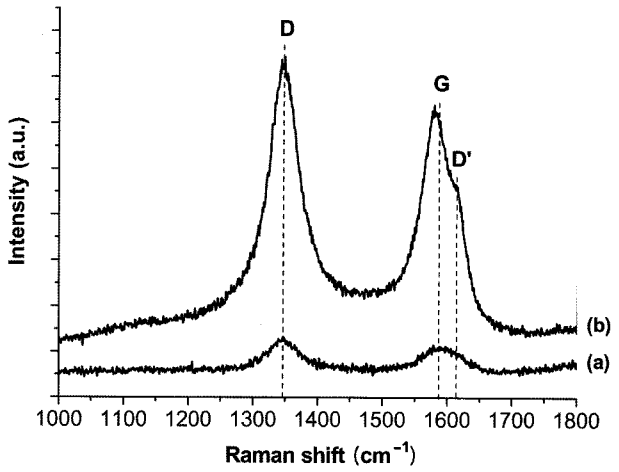

Figure 3. Raman spectra of pristine MWNTs and MWNT-COOH: pristine MWNTs (a) and MWNT-COOH (b) on the slide glass (Raman spectrometer with 532-nm excitation source).

The solution of palladium (II) acetate in methanol is used for producing palladium nanoparticles with no POSS-NH_3^+ on Si-substrates and the turbid solution containing POSS-NH_3^+ and palladium (II) acetate is used for producing Pd-POSS on Si-substrates. To observe SEM images, both of the solutions are allowed to evaporate the solvent. Figure 4(a) shows individual palladium nanoparticles with a diameter of 3 nm. On the other hand, for Pd-POSS, Figure 4(b) and Figure 5 show the formation of spherical aggregates with a diameter of 40-60 nm and no individual palladium nanoparticles. These results might be attributed to the structure and functionality of POSS-NH_3^+ for the formation of the spherical aggregates.[56] Normally, the particles tend to grow into a spherical shape to minimize their surface energy. In this system, we could estimate that the self-organized spherical templates

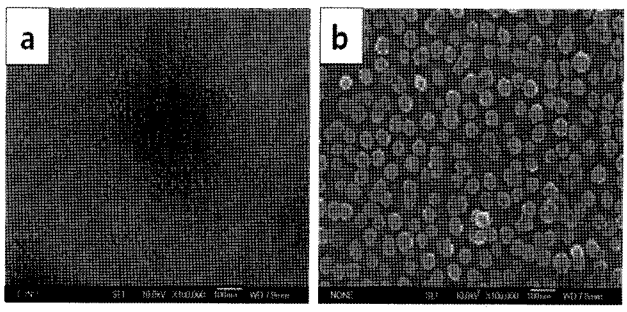

Figure 4. FE-SEM images of palladium nanoparticles (a) and Pd-POSS (b).

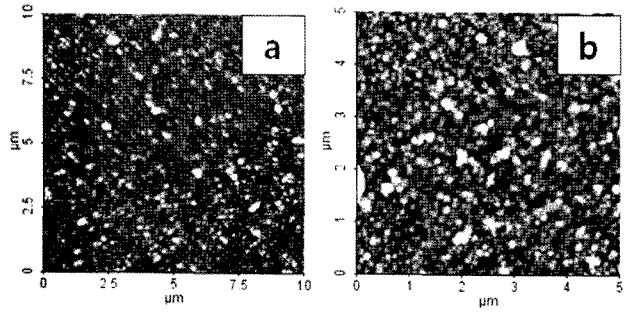

Figure 5. Tapping-mode AFM images of Pd-POSS (a and b).

consisting of palladium ions and POSS-NH_3^+ became spherical by the same reason.

For Figure 6, samples were poduced by immersing the amine-functionalized Si-substrates in DDI water solution of pristine MWNTs and MWNT-COOH for 12 h, and then both of the Si-substrates were washed with DDI water at 3 times to remove the unreacted MWNTs. The pristine MWNTs were not observed on the amine-functionalized Si-substrates in Figure 6(a). On the other hand, Figure 6(b), 6(c), and Figure 7 showed that MWNT-COOH were well dispersed on the amine-functionalized Si-substrates. From the above results, it was confirmed that MWNT-COOH were coated on the amine-functionalized substrates by self-assembly reaction.

Si-substrates coated with the MWNT-COOH were immersed in methanol solution of palladium (II) acetate or in methanol solution of POSS-NH_3^+ and palladium (II) acetate, respectively. And then substrates were washed sufficiently with methanol. The surfaces of the Si-substrates were studied by SEM. It was observed that there was no deposition of individual palladium nanoparticles with no POSS-NH_3^+ on the MWNT-COOH of Si-substrates as shown in Figure 8(a), whereas from Figure 8(b) and Figure 9, it was evident that Pd-POSS were deposited well on the MWNT-COOH of Si-

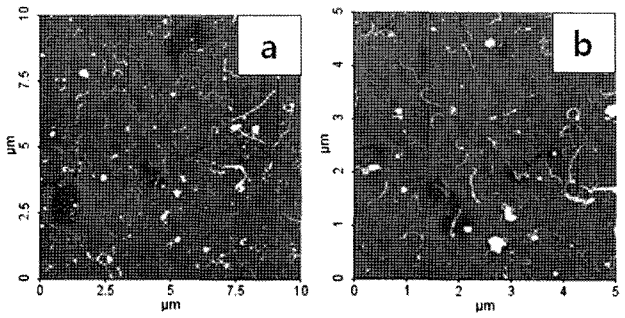

Figure 7. Tapping-mode AFM images of MWNT-COOH on the amine-functionalized substrates (a and b).

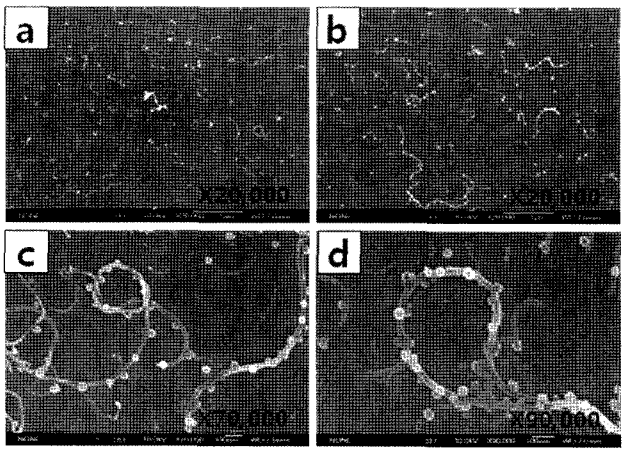

Figure 8. FE-SEM images of MWNT-COOH on the amine-functionalized substrates (no deposition of palladium nanoparticles) (a) and Pd-MWNT nanocomposites (b, c, and d).

substrates. Pd-POSS deposited on the MWNT-COOH have size distributions in the range of 40-60 nm and are homogeneously dispersed on the surfaces of the MWNT-COOH. These results indicate that hybrid nanocomposites don't form between individual palladium nanoparticles and MWNT-

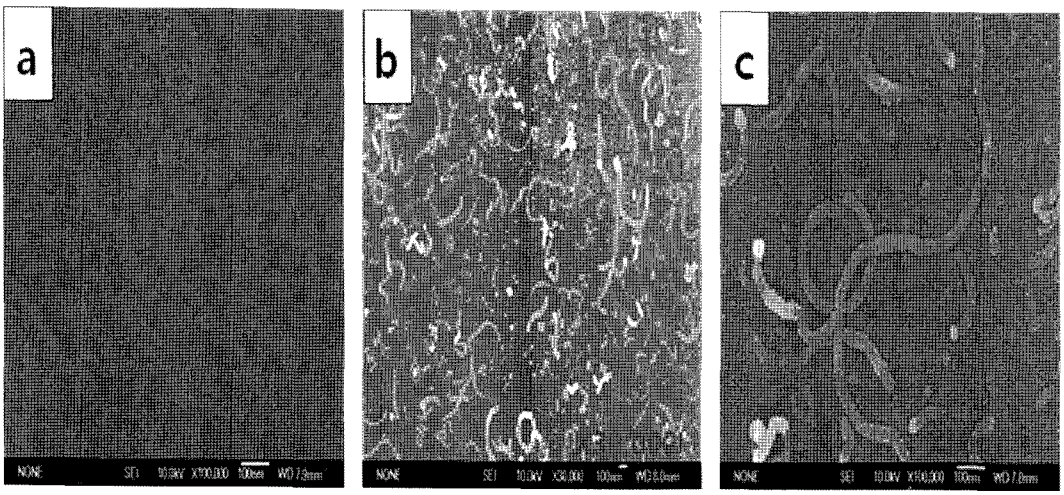

Figure 6. FE-SEM images of pristine MWNTs (a) and MWNT-COOH on the amine-functionalized substrates (b and c).

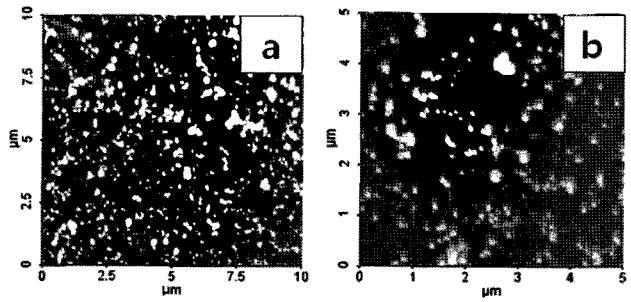

Figure 9. Tapping-mode AFM images of Pd-MWNT nanocomposites (a and b).

COOH but between the spherical aggregates of Pd-POSS and MWNT-COOH. This reason is that the ionic interactions between positively charged Pd-POSS and negatively charged MWNT-COO^- play an important role for the formation of hybrid nanocomposites. As shown in Figure 9, the AFM study reveals the presence of Pd-POSS deposition on the MWNT-COOH in good agreement with the SEM images in Figure 8.

The composition of Pd-POSS, MWNT-COOH, and Pd-MWNT nanocomposites were confirmed by X-ray energy dispersive spectroscopy (EDX) analysis. Figure 10(a) and 10(b) show the palladium peak at 2.85 keV and the carbon peak at 0.28 keV derived from Pd-POSS and MWNT-COOH, respectively. In Figure 10(c), after the synthesis of Pd-MWNT

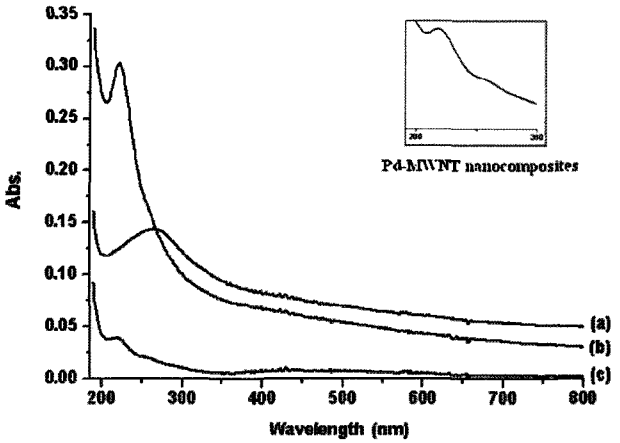

Figure 11. UV-vis absorption spectra of MWNT-COOH (a), Pd-POSS (b), and Pd-MWNT nanocomposites (c).

nanocomposites, the peaks at 0.28 keV (carbon), 2.84 keV (palladium), and 3.55 keV (palladium) were obtained in the spectra.

An additional evidence of the formation of Pd-MWNT nanocomposites was investigated by UV-vis spectroscopy (Figure 11). The strong absorption band of Pd-POSS was observed at 221 nm and the broad absorption band at 263 nm was observed for MWNT-COOH. The both absorption peaks at 220 nm and 264 nm were present for Pd-MWNT

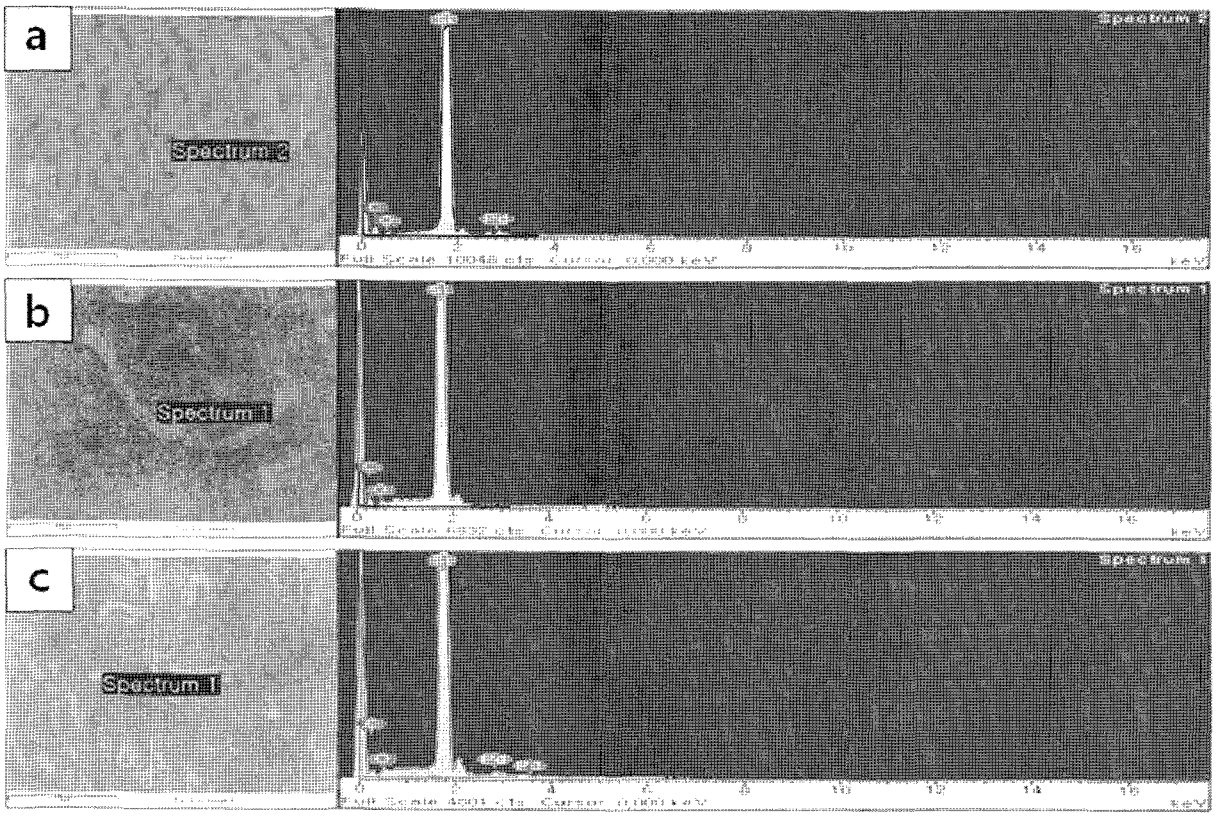

Figure 10. FE-SEM image and EDX spectrum of Pd-POSS (a), MWNT-COOH (b), and Pd-MWNT nanocomposites (c).

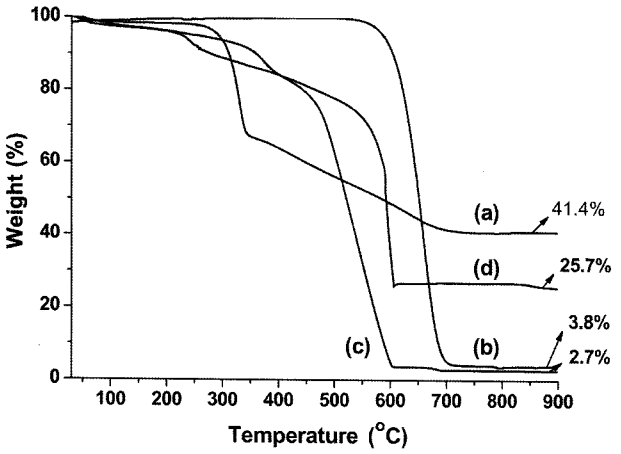

Figure 12. TGA curves of Pd-POSS (a), pristine MWNTs (b), MWNT-COOH (c), and Pd-MWNT nanocomposites (d) (in atmosphere).

nanocomposites, indicating that MWNT-COOH were successfully incorporated into the spherical aggregates of Pd-POSS with a diamater of 40-60 nm.

In order to compare the thermal stability of pristine MWNTs, MWNT-COOH, Pd-POSS, and Pd-MWNT nanocomposites, thermal analysis was carried out by TGA measurements as shown in Figure 12. Figure 12(b) and 12(c) show that the difference from the thermal decomposition between pristine MWNTs and MWNT-COOH is attributed to the increase of organic functional group on the surfaces of pristine MWNTs by the chemical modification under acidic condition. The weight (ca. 25.7 wt%) of the residue obtained from Pd-MWNT nanocomposites is larger than that (ca. 2.7 wt%) obtained from the MWNT-COOH as shown in Figure 12(d). This results suggest that Pd-POSS are well deposited on the MWNT-COOH. Furthermore, the thermal stability of Pd-MWNT nanocomposites is higher than that of the MWNT-COOH and Pd-POSS.

Conclusions

In summary, we have developed a new approach for hybrid nanocomposites of Pd-POSS containing POSS-NH_3^+ and MWNT-COOH through the self-assembly method via ionic interactions as physical bonding interaction. Positively charged Pd-POSS were well deposited to negatively charged MWNT-COOH on silicon wafer due to the opposite charged surfaces. Ionic interactions between positively charged Pd-POSS and negatively charged MWNT-COO^- are the driving force for the formation of nanocomposites of Pd-POSS and MWNT-COOH. The spherical aggregates of Pd-POSS with a diameter of 40-60 nm were successfully attached to the dispersed MWNT-COOH on the amine-functionalized substrates. The obtained hybrid nanocomposites show the enhanced thermal stability as compared to MWNT-COOH and Pd-POSS. MWNTs modified with Pd-POSS provide a promising class of new material for fabricating high-performance hydrogen sensing devices.

Acknowledgements. This work was supported by the Korean Research Foundation Grant funded by the Korean Government (MOEHRD) (KRF-2008-D00165) and the Ministry of Education, Science Technology (MEST) and Korea Industrial Technology Foundation (KOTEF) through the Human Resource Training Project for Regional Innovation.

References

(1) M. C. Daniel and D. Astruc, *Chem. Rev.*, **104**, 293 (2004).
(2) A. Henglein, *Chem. Rev.*, **89**, 1861 (1989).
(3) A. C. Templeton, W. P. Wuelfing, and R. W. Murray, *Acc. Chem. Res.*, **33**, 27 (2000).
(4) G. Schmid and B. Corain, *Eur. J. Inorg. Chem.*, 3081 (2003).
(5) R. Schenhar, T. B. Norsten, and V. M. Rotello, *Adv. Mater.*, **17**, 657 (2005).
(6) C. N. R. Rao, G. U. Kulkarni, P. J. Thomas, and P. P. Edwards, *Chem. Soc. Rev.*, **29**, 27 (2000).
(7) C. A. Mirkin, R. L. Letsinger, R. C. Mucic, and J. J. Storhoff, *Nature (London, U.K.)*, **382**, 607 (1996).
(8) S. Mann, W. Shenton, M. Li, S. Connolly, and D. Fitzmaurice, *Adv. Mater.*, **12**, 147 (2000).
(9) T. Teranishi, M. Haga, Y. Shiozawa, and M. Miyake, *J. Am. Chem. Soc.*, **122**, 4237 (2000).
(10) S. Mandal, A. Gole, N. Lala, R. Gonnade, V. Ganvir, and M. Sastry, *Langmuir*, **17**, 6262 (2001).
(11) E. Adachi, *Langmuir*, **16**, 6460 (2000).
(12) J. Jin, T. Iyoda, C. Cao, Y. Song, L. Jiang, T. Li, and D. Zhu, *Angew. Chem. Int. Ed.*, **40**, 2135 (2001).
(13) I. Hussain, Z. Wang, A. I. Cooper, and M. Brust, *Langmuir*, **22**, 2938 (2006).
(14) W. A. De Heer, A. Chatelain, and E. Ugarte, *Science*, **270**, 1179 (1995).
(15) P. M. Ajayan, O. Stephan, C. Collix, and D. Trauth, *Science*, **265**, 1212 (1994).
(16) P. Chen, X. Wu, J. Lin, and K. L. Tan, *Science*, **285**, 91 (1999).
(17) J. Kong, N. R. Franklin, C. W. Zhou, M. G. Chapline, S. Peng, K. J. Cho, and H. J. Dai, *Science*, **287**, 622 (2000).
(18) S. D. Park, W. Xu, C. Chung, and Y. Kwon, *Macromol. Res.*, **16**, 155 (2008).
(19) I. Park, M. Park, J. Kim, H. Lee, and M. S. Lee, *Macromol. Res.*, **15**, 498 (2007).
(20) B. S. Kim, K. D. Suh, and B. Kim, *Macromol. Res.*, **16**, 76 (2008).
(21) S. H. Lee, J. S. Park, C. M. Koo, B. K. Lim, and S. O. Kim, *Macromol. Res.*, **16**, 261 (2008).
(22) K. H. Kim and W. H. Jo, *Macromol. Res.*, **16**, 749 (2008).
(23) N. S. Lawrence, R. P. Deo, and J. Wang, *Electroanalysis*, **17**, 65 (2005).
(24) K. F. Fu and Y. P. Sun, *J. Nanosci. Nanotechnol.*, **3**, 351 (2003).
(25) Y. P. Sun, K. F. Fu, Y. Lin, and W. J. Huang, *Acc. Chem. Res.*, **35**, 1096 (2002).
(26) J. Liu, A. G. Rinzler, H. J. Dai, J. H. Hafner, R. K. Bradley, P. J. Boul, A. Lu, T. Iverson, K. Shelimov, C. B. Huffman, F.

Rodriguez-Macias, Y. S. Shon, T. R. Lee, D. T. Colbert, and R. E. Smalley, *Science*, **280**, 1253 (1998).
(27) W. Z. Li, C. H. Liang, W. J. Zhou, J. S. Qiu, Z. H. Zhou, G. Q. Sun, and Q. Xin, *J. Phys. Chem. B*, **107**, 6292 (2003).
(28) J. Kong, M. G. Chapline, and H. J. Dai, *Adv. Mater.*, **13**, 1384 (2001).
(29) A. Bezryadin, C. N. Lau, and M. Tinkham, *Nature*, **404**, 971 (2000).
(30) B. Xue, P. Chen, Q. Hong, J. Y. Lin, and K. L. Tan, *J. Mater. Chem.*, **11**, 2378 (2001).
(31) J. Li, M. Moskovits, and T. L. Haslett, *Chem. Mater.*, **10**, 1963 (1998).
(32) B. R. Azamian, K. S. Coleman, J. J. Davis, N. Hanson, and M. L. H. Green, *Chem. Commun.*, 366 (2002).
(33) Y. Mu, H. Liang, J. Hu, L. Jiang, and L. Wan, *J. Phys. Chem. B*, **109**, 22212 (2005).
(34) G. P. Jin, Y. F. Ding, and P. P. Zheng, *J. Power Sources*, **166**, 80 (2007).
(35) C. H. Yen, K. Shimizu, Y. Y. Lin, F. Bailey, I. F. Cheng, and C. M. Wai, *Energy Fuels*, **21**, 2268 (2007).
(36) J. Shi, Z. Wang, and H. L. Li, *J. Nanoparticle Res.*, **8**, 743 (2006).
(37) S. Banerjee, M. G. C. Kahn, and S. S. Wong, *Chem. Eur. J.*, **9**, 1898 (2003).
(38) J. Chattopadhyay, A. K. Sadana, F. Liang, J. M. Beach, Y. Xiao, R. H. Hauge, and W. E. Billups, *Org. Lett.*, **7**, 4067 (2005).
(39) P. F. Ho and K. M. Chi, *Nanotechnology*, **15**, 1059 (2004).
(40) Y. Hayashi, T. Tokunaga, S. Toh, W. J. Moon, and K. Kaneko, *Diamond. Relat. Mater.*, **14**, 790 (2005).
(41) G. Guella, C. Zanchetta, B. Patton, and A. Miotello, *J. Phys. Chem. B*, **110**, 17024 (2006).
(42) A. Corma, H. Garcia, and A. Primo, *J. Catal.*, **241**, 123 (2006).
(43) Y. Fukai and H. Sugimoto, *Adv. Phys.*, **34**, 263 (1985).
(44) N. Watari, S. Ohnishi, and Y. Ishii, *J. Phys. Condens. Matter.*, **12**, 6799 (2000).
(45) S. Kishore, J. A. Nelson, J. H. Adair, and P. C. Eklund, *J. Alloy Compd.*, **389**, 234 (2005).
(46) S. Horinouchi, Y. Yamanoi, T. Yonezawa, T. Mouri, and H. Nishihara, *Langmuir*, **22**, 1880 (2006).
(47) A. Anson, E. Lafuente, E. Urriolabeitia, R. Navarro, A. M. Benito, W. K. Maser, and M. T. Martinez, *J. Phys. Chem. B*, **110**, 6643 (2006).
(48) J. Evans, *Chem. World*, **3**, 16 (2006).
(49) G. Korotcenkov, V. Brinzari, Y. Boris, M. Ivanova, J. Schwank, and J. Morante, *Thin Solid Films*, **436**, 119 (2003).
(50) T. Skala, K. Veltruska, M. Moroseac, I. Matolinova, A. Cirera, and V. Matolin, *Surf. Sci.*, **566**, 1217 (2004).
(51) Y. Suda, H. Kawasaki, J. Namba, K. Iwatsuji, K. Doi, and K. Wada, *Surf. Coat. Technol.*, **174**, 1293 (2003).
(52) S. Toh, K. Kaneko, Y. Hayashi, T. Tokunaga, and W. J. Moon, *J. Electron. Microsc.*, **53**, 149 (2004).
(53) Y. J. Lu, J. Li, J. Han, H. T. Ng, C. Binder, C. Partridge, and M. Meyyappan, *Chem. Phys. Lett.*, **391**, 344 (2004).
(54) F. J. Feher and K. D. Wyndham, *Chem. Commun.*, 323 (1998).
(55) C. Gao, Y. Z. Jin, H. Kong, R. L. D. Whitby, S. F. A. Acquah, G. Y. Chen, H. Qian, A. Hartschuh, S. R. P. Silva, S. Henley, P. Fearon, H. W. Kroto, and D. R. M. Walton, *J. Phys. Chem. B*, **109**, 11925 (2005).
(56) K. Naka, H. Itoh, and Y. Chujo, *Nano Lett.*, **2**, 1183 (2002).